

Multichannel pseudogap Kondo model: Large- N solution and quantum-critical dynamics

Matthias Vojta

Theoretische Physik III, Elektronische Korrelationen und Magnetismus, Universität Augsburg, 86135 Augsburg, Germany
(February 5, 2001)

We discuss a multichannel $SU(N)$ Kondo model which displays non-trivial zero-temperature phase transitions due to a conduction electron density of states vanishing with a power law at the Fermi level. In a particular large- N limit, the system is described by coupled integral equations corresponding to a dynamic saddle point. We exactly determine the universal low-energy behavior of spectral densities at the scale-invariant fixed points, obtain anomalous exponents, and compute scaling functions describing the crossover near the quantum-critical points. We argue that our findings are relevant to recent experiments on impurity-doped d -wave superconductors.

The Kondo effect in metals is a well studied phenomenon in many-body physics. The low-energy physics is completely determined by a single energy scale, the Kondo temperature T_K , and the impurity spin is fully quenched in the low-temperature limit, $T \ll T_K$ [1]. The standard picture of the Kondo effect has to be revised if the conduction band density of states (DOS) vanishes identically at the Fermi energy [2–6]. This is the case in so-called pseudogap systems with a power-law DOS $\rho(\epsilon) \sim |\epsilon|^r$ ($r > 0$) which arises in one-dimensional interacting systems, in certain zero-gap semiconductors, and in systems with long-range order where the order parameter has nodes at the Fermi surface, *e.g.*, p - and d -wave superconductors ($r = 2$ and 1). Of special interest are high- T_c cuprate superconductors, where indeed non-trivial Kondo-like behavior has been observed associated with the magnetic moments induced by non-magnetic Zn impurities [7].

The pseudogap Kondo problem has attracted a lot of attention during the last decade. A number of studies [2,3] including the initial work by Withoff and Fradkin employed a slave-boson large- N technique; further progress and insight came from numerical renormalization group (NRG) calculations [4–6] and the local moment approach [8]. The general picture arising from these studies is that there exists a zero-temperature phase transition at a critical Kondo coupling, J_c , below which the impurity spin is unscreened even at lowest temperatures. Also, the behavior depends sensitively on the presence or absence of particle-hole (p-h) symmetry: in the p-h symmetric case there is no complete screening even for $J_K > J_c$. A comprehensive discussion of possible fixed points and their thermodynamic properties has been given by Gonzalez-Buxton and Ingersent [6] based on the NRG approach. Spectral properties of the pseudogap Kondo model have so far been investigated for the p-h symmetric case only [5,8], and the knowledge about the quantum-critical dynamics is limited. Importantly, recent advances in scanning tunneling microscopy (STM) have made it possible to directly observe local spectral properties of impurities in superconductors [9].

The purpose of this paper is to provide an exact low-

energy solution of the pseudogap Kondo problem in a certain large- N limit [10,11] which is appropriate for obtaining dynamical properties. We shall determine anomalous exponents and spectral densities at the fixed points of interest, and describe the crossovers in the vicinity of quantum-critical points. The critical fixed points are found to have exponents varying continuously with the pseudogap exponent r . To our knowledge, our study represents the first critical theory of the pseudogap Kondo transition in the presence of p-h asymmetry.

We begin by describing the generalized multichannel Kondo problem, characterized by K channels of conduction electrons and a spin symmetry group extended from $SU(2)$ to $SU(N)$. The choice of the $SU(N)$ representation for the impurity spin \hat{S} qualitatively influences the phase diagram in the large- N limit. For $r = 0$, a symmetric (bosonic) representation leads to both underscreened and overscreened [12,13] phases with an exactly screened phase in between [10], whereas an antisymmetric representation only allows for an overscreened situation [11]. A second crucial difference is that the bosonic large- N limit contains a generic p-h asymmetry which prevents a study of a p-h symmetric model. Therefore, we choose an antisymmetric representation [11] for \hat{S} , corresponding to a Young tableau with a single column of Q boxes. The $N^2 - 1$ traceless components of \hat{S} can be written in terms of N auxiliary fermions, f_ν , as $S_{\nu\mu} = f_\nu^\dagger f_\mu - Q \delta_{\nu\mu}/N$, together with the constraint $\sum_\nu f_\nu^\dagger f_\nu = Q$. The conduction electrons transform under the fundamental representation of $SU(N)$, and carry a channel (flavor) index $i = 1, \dots, K$ and $SU(N)$ spin index $\nu = 1, \dots, N$. The Hamiltonian of the model reads:

$$H = \sum_{\mathbf{k}\nu} \epsilon_{\mathbf{k}} c_{\mathbf{k}\nu}^\dagger c_{\mathbf{k}\nu} + J_K \sum_{\mathbf{k}\mathbf{k}'\nu\mu} S_{\nu\mu} c_{\mathbf{k}\mu}^\dagger c_{\mathbf{k}'\nu} \quad (1)$$

The fermionic bath is assumed to have a power law DOS at low energies; for simplicity we use a model DOS given by $\rho(\epsilon) = \rho_0 |\epsilon/D|^r$ for $|\epsilon| < D$.

For $r = 0$, it is known that weak antiferromagnetic coupling J_K grows under renormalization for $K \geq 2$ and any N , Q , and there is a stable intermediate-coupling non-Fermi-liquid fixed point associated with overscreen-

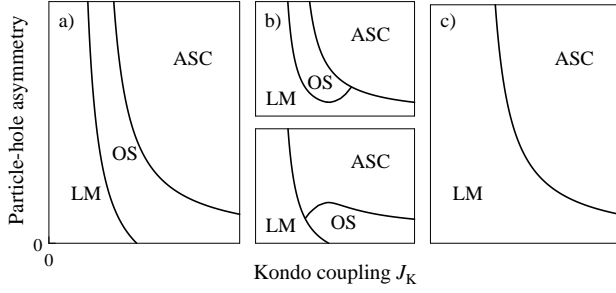


FIG. 1. Schematic phase diagrams of the multichannel pseudogap Kondo model as function of the Kondo coupling J_K and the particle-hole asymmetry (*e.g.* potential scattering), for pseudogap exponents r with a) $0 < r < r_{\min}^*$, b) $r_{\min}^* < r < r_{\max}^*$ for $\gamma > \gamma_c$ (top) and $\gamma < \gamma_c$ (bottom), $\gamma_c \simeq 0.8$, c) $r > r_{\max}^*$.

ing of the impurity spin. For $r > 0$, we find that the situation is different, and a number of phases appear: (i) A local moment (LM) regime is reached for weak initial coupling. Here J_K flows to zero, and the impurity is unscreened. (ii) An overscreened phase (OS) is found for $0 < r < r_{\max}^*$ and $J_{c1} < J_K < J_{c2}$, it is a natural generalization of the $r = 0$ overscreened fixed point. (iii) There is a new asymmetric strong-coupling (ASC) phase which exists for $r > 0$, and is reached only for $J_K > J_{c2}$ and a sufficient amount of p-h symmetry breaking. Qualitative phase diagrams are shown Fig. 1; the important case of $r = 1$ corresponds to Fig. 1c.

We now proceed with the analysis of the model in the large- N limit which has been introduced in Refs. [10,11]. We set $K = \gamma N$, $J_K = J/N$, and take the limit $N \rightarrow \infty$ keeping γ and J fixed. The important difference of the present large- N limit to the usual non-crossing approximation (NCA) [14] is the treatment of the occupation constraint: here we set $Q = q_0 N$ and keep q_0 fixed. The advantage is twofold: we can achieve p-h symmetry with $Q = N/2$, and in the large- N limit the dynamics of the system is determined by a true (time-dependent) saddle point [10,11]. (Formally, results corresponding to $Q = 1$ as in Ref. [14] are obtained here in the limit $q_0 \rightarrow 0$.) The Kondo interaction in Eq. (1) can be decoupled in each channel by auxiliary bosonic fields $B_i(\tau)$, conjugate to the amplitude $\sum_\nu c_{i\nu}^\dagger(\tau) f_\nu(\tau)$. The constraint is implemented with a Lagrange multiplier field $\lambda(\tau)$. One finds the following integral equations for the fermionic and bosonic Green's functions $G_f(\tau) = -\langle T_\tau f_\nu(\tau) f_\nu^\dagger(0) \rangle$, $G_B(\tau) = \langle T_\tau B_i(\tau) B_i^\dagger(0) \rangle$:

$$\Sigma_f(\tau) = \gamma G_0(\tau) G_B(\tau), \quad \Sigma_B(\tau) = -G_0(-\tau) G_f(\tau), \quad (2)$$

with the self-energies Σ_f and Σ_B defined by:

$$G_f^{-1}(i\omega_n) = i\omega_n + \lambda - \Sigma_f(i\omega_n) \quad (3)$$

$$G_B^{-1}(i\nu_n) = \frac{1}{J} - \Sigma_B(i\nu_n). \quad (4)$$

In these expressions $\omega_n = (2n+1)\pi/\beta$ and $\nu_n = 2n\pi/\beta$ denote fermionic and bosonic Matsubara frequencies.

The third saddle point equation fixes the impurity “occupation” and thus determines λ :

$$G_f(\tau = 0^-) = \frac{1}{\beta} \sum_n G_f(i\omega_n) e^{i\omega_n 0^+} = q_0. \quad (5)$$

Eqs. (2,3,4) are identical in structure to the usual NCA equations, but the physics is changed by the constraint eq. (5) which keeps track of the choice of the impurity spin representation. With a symmetric conduction band DOS, the model is p-h symmetric (invariant under $f_\nu^\dagger \leftrightarrow f_\nu$ and $c_{\mathbf{k}i\nu}^\dagger \leftrightarrow c_{\mathbf{k}i\nu}$) for $q_0 = 1/2$. P-h symmetry can be broken at the impurity spin ($q_0 \neq 1/2$) as well as in the environment (potential scattering or doping), both leading to similar effects.

An important dynamic observable is the conduction electron T-matrix $T(\omega)$ (which corresponds to the impurity Green's function for an impurity Anderson model), given by the convolution of G_f and G_B , so its Fourier transform is $T(\tau) = -(1/N) G_f(\tau) G_B(-\tau)$. Local susceptibilities for the spin and channel degrees of freedom are obtained by $\chi_{\text{loc,sp}} = -\int_0^\beta d\tau G_f(\tau) G_f(-\tau)$ and $\chi_{\text{loc,ch}} = \int_0^\beta d\tau G_B(\tau) G_B(-\tau)$; these have to be distinguished from the impurity contributions $\chi_{\text{imp,sp,ch}}$ to the response to a *global* (spin or channel) field.

We now turn to a detailed analysis of the low-energy, low-temperature behavior of the above equations. In a first step, we analyze possibly existing scale-invariant fixed points where the Green's functions follow power laws at small frequencies. It is important to note that *any* continuous quantum phase transition (as well as other possible intermediate coupling fixed points) must be described by such behavior. The constant terms in Eqs. (3,4) have to vanish, $\lambda - \Sigma_f(i0^+) \rightarrow 0$, $1/J - \Sigma_B(i0^+) \rightarrow 0$ as $T \rightarrow 0$ [11]. A power-law ansatz $G_B(\tau) \sim A_B/\tau^{2\Delta_B}$, $G_f(\tau) \sim A_f/\tau^{2\Delta_f}$ for the Green's functions in the regime $1/T^* \ll \tau \ll \beta \rightarrow \infty$ (where T^* is a crossover temperature) is equivalent to low-energy spectral densities

$$\rho_{f,B}(\omega \rightarrow 0^\pm) \sim \frac{A_{f,B,\pm}}{(\pm\omega)^{1-2\Delta_{f,B}}}, \quad (6)$$

which have the same power-law exponent, but different prefactors A_\pm , for $\omega > 0$ and $\omega < 0$. Inserting these Green's functions into Eqs. (2,3,4) one finds the following equations for the exponents:

$$2\Delta_f + 2\Delta_B = 1 - r, \quad \gamma \frac{(1 - 2\Delta_B) \sin 2\pi\Delta_B}{\sin^2 \pi\Delta_B + \sinh^2 \alpha/2} = \frac{(1 - 2\Delta_f) \sin 2\pi\Delta_f}{\cos^2 \pi\Delta_f + \sinh^2 \alpha/2}. \quad (7)$$

Here, α is a spectral asymmetry parameter defined by $\exp(\alpha) = A_{f,-}/A_{f,+} = -A_{B,-}/A_{B,+}$. For $r = 0$, α drops out, and there is a single solution with non-trivial exponents, $2\Delta_f = 1/(1+\gamma)$, $2\Delta_B = \gamma/(1+\gamma)$, which describes an infrared stable fixed point corresponding to

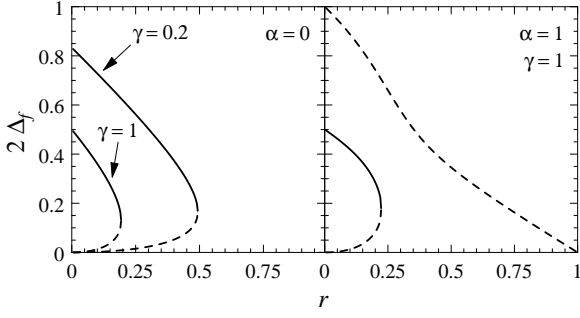


FIG. 2. Values of the exponent $2\Delta_f$ at the scale-invariant fixed points, obtained from Eq. (7), as function of r . Solid: infrared stable fixed points (OS). Dashed: unstable fixed points (quantum phase transitions). Left: particle-hole symmetric case $\alpha = 0$. Right: with particle-hole asymmetry. The disappearance of the stable OS solution marks the value of $r^*(\alpha)$. We find $r_{\min}^*, r_{\max}^* \rightarrow 1$ for $\gamma \rightarrow 0$, $r_{\min}^* \simeq 0.19$, $r_{\max}^* \simeq 0.29$ for $\gamma = 1$, and $r_{\min}^*, r_{\max}^* \rightarrow 0$ for $\gamma \rightarrow \infty$. (In the single-channel SU(2) case, $r^* = \frac{1}{2}$, whereas $N = K = 2$ gives $r^* \simeq 0.23$ [6].)

an overscreened spin [11]. In contrast, the behavior for $0 < r \leq 1$ is much richer, and is illustrated in Figs. 1 and 2. For small r and $\alpha \neq 0$, one finds three solutions, one infrared stable representing the OS phase, and two unstable corresponding to the quantum phase transitions from OS to LM and ASC. With increasing r , two solutions disappear at $r^*(\alpha)$, leaving a single unstable solution for the direct transition between the LM and ASC phases. In the p-h symmetric case ($\alpha=0$), the unstable solution for the transition to ASC is absent. Therefore, no scale-invariant solution is found for $r > r^*(0)$: the p-h symmetric system here always flows to the LM weak coupling phase. The critical value $r^*(\alpha)$ is bounded, $r_{\min}^* < r^* < r_{\max}^*$. From the presence or absence of intermediate coupling fixed points one can infer phase diagrams as in Fig. 1; these are also well borne out by our numerical studies of Eqs. (2,3,4). In the narrow range $r_{\min}^* < r < r_{\max}^*$, the existence of the OS phase depends on the amount of p-h symmetry breaking, Fig. 1b.

The $N = K = 2$ version of the overscreened pseudogap Kondo model has been studied earlier by NRG [6], with results somewhat different from the large- N limit. The $N = K = 2$ model has a single r^* value, no ASC region for $r < r^* \simeq 0.23$, and a minimal potential scattering value to reach ASC for $r > r^*$. Some of these differences arise from the fact that the $N = K = 2$ case exhibits isolated critical fixed points, whereas the scale-invariant large- N solutions actually correspond to continuous *lines of fixed points*, parametrized by the low-energy spectral asymmetry α , which is determined by the symmetry-breaking parameters of the model.

The universal low-energy behavior of the T-matrix at the scale-invariant fixed points is readily obtained from the convolution of G_f and G_B , its spectral density $\rho_T(\omega \rightarrow 0)$ diverges as $A_T|\omega|^{-r}$. Notably, the prefactors for both signs of ω are equal here, *i.e.*, the asymmetry

described by α disappears in the scaling limit [11]. Furthermore, the amplitude A_T in the OS phase is independent of J , this is the analog of Friedel's sum rule. The scaling forms of the *finite-temperature* spectral densities can be determined [11] from the $T = 0$ quantities (6) by applying a conformal transformation $z = \exp(i2\pi\tau/\beta)$. Low-temperature thermodynamic quantities can now be calculated, *e.g.*, the local spin susceptibility [11,14] follows $\chi_{\text{loc,sp}} \sim 1/T^{1-4\Delta_f}$ for $4\Delta_f < 1$, $\chi_{\text{loc,sp}} \sim \ln(1/T)$ for $4\Delta_f = 1$, and $\chi_{\text{loc,sp}} \sim \text{const}$ otherwise; similar results hold for $\chi_{\text{loc,ch}}$ in terms of Δ_b .

In a second step, we discuss possible non-scale-invariant fixed points of the system (which are absent at $r = 0$): the local moment (LM) and the asymmetric strong coupling (ASC) fixed point. These solutions of Eqs. (2,3,4) appear if the $T = 0$ “compensation” of the constant terms in Eqs. (3,4) is not realized.

For the LM fixed point, reached for small Kondo coupling, it is important to notice that $\Sigma_B(i0+)$ is bounded from above for $r > 0$ and cannot compensate large $1/J$ values (the corresponding integral is infrared divergent for $r = 0$). Hence, there is no power-law solution for J smaller than a critical J_{c1} . A constant term in G_B^{-1} implies a δ -peak in the $T = 0$ fermion spectral density; furthermore the spectral asymmetry flows to zero in the scaling limit, leading to $\rho_f(\omega) \sim \delta(\omega)$. This is equivalent to an unscreened spin: the local spin susceptibility follows a Curie law for $T \rightarrow 0$. The “local moment” $T\chi_{\text{loc,sp}}$ is reduced from its free spin value, but $T\chi_{\text{imp,sp}}$, measuring the *total* impurity-induced Curie contribution to the uniform susceptibility, is that of a free spin, *i.e.*, part of the moment is carried by the surrounding conduction electrons due to the residual coupling mediated by G_B .

The ASC fixed point is reached at sufficient particle-hole asymmetry and Kondo coupling. Here, $\lambda - \Sigma_f(i0+)$ does not vanish for $T \rightarrow 0$. This leads to a δ -peak in the auxiliary boson spectral density, $\rho_B(\omega) \sim \pm\delta(\omega - 0^\pm)$ [the sign depending on $\text{sgn}(q_0 - 1/2)$], which implies maximal spectral asymmetry in the scaling limit. The channel susceptibility diverges like $1/T$, and the system has a free “moment” in the channel (flavor) degrees of freedom, also leading to a residual $T = 0$ entropy. In contrast, the spin is completely screened, $\chi_{\text{imp,sp}}, \chi_{\text{loc,sp}} \rightarrow \text{const}$. The ASC phase can be understood as $(N - Q)$ conduction electrons bound to the impurity; for $N = K = 2$ this is equivalent to a spin singlet, channel doublet state [6].

For both the LM and ASC fixed points, the spectral density $\rho_T(\omega)$ of the T-matrix behaves as $|\omega|^r$ at small frequencies, and the spectral asymmetry disappears in the scaling limit of ρ_T .

At this point we briefly comment on the case $r \geq 1$: the OS phase disappears for all γ ; in the presence of particle-hole asymmetry a transition between LM and ASC is still possible. For $r = 1$ the above power law analysis remains valid, but has to be supplemented with logarithmic corrections. For $r > 1$ the critical power law

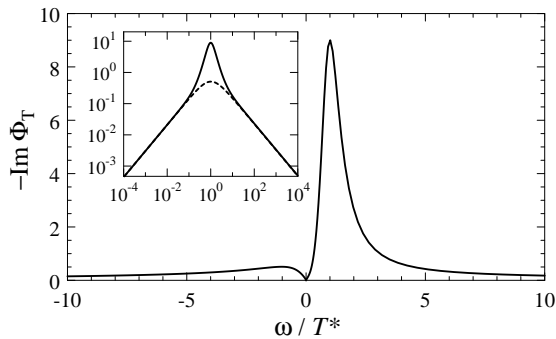


FIG. 3. Zero-temperature scaling function Φ_T for the conduction electron T-matrix at $r = 0.8$, $\gamma = 1$, $q_0 = 0.1$, describing the crossover from the ASC behavior at low energies to quantum criticality at high energies. Inset: Same on log-log scale, showing both $\bar{\omega} > 0$ (solid) and $\bar{\omega} < 0$ (dashed).

at the LM-ASC transition is replaced by $\rho_T \sim |\omega|^{r-2}$.

After having described the fixed points we now turn to the universal behavior near the quantum phase transitions. In the vicinity of each critical point, one can define an energy scale T^* , which vanishes at the transition, and defines the crossover energy above which quantum-critical behavior is observed [15]. From the above low-energy analysis one can deduce the dependence of T^* on the reduced coupling, $j = (J - J_c)/J_c$, measuring the distance from the critical point at J_c . Approaching the LM-OS or LM-ASC transition from small J we have $T^* \sim (-j)^{1/r}$, from large J we find $T^* \sim j^{1/(r+2\Delta_{f,cr})}$ where $\Delta_{f,cr}$ is the anomalous fermion exponent at the critical fixed point. Similarly, we have $T^* \sim (-j)^{1/(r+2\Delta_{f,os})}$ and $T^* \sim j^{1/(r+2\Delta_{f,cr})}$ if we approach the OS-ASC transition from below or above, respectively. The local susceptibilities are easily derived, *e.g.*, in the ASC phase we have $\chi_{loc,sp}(T=0) \sim T^{*(4\Delta_{f,cr}-1)} \sim j^{-\bar{\gamma}}$ with $\bar{\gamma} = (1 - 4\Delta_{f,cr})/(r + 2\Delta_{f,cr})$.

Near a critical point all observables show scaling behavior as function of T/T^* and ω/T^* ($k_B = 1$). For instance, the T-matrix obeys the scaling form

$$T(\omega) = \frac{\mathcal{A}}{T^{*(1-\eta_T)}} \Phi_T\left(\frac{\omega}{T^*}, \frac{T}{T^*}\right), \quad (8)$$

where \mathcal{A} is an amplitude prefactor, $\eta_T = 1 - r$ is the anomalous exponent, and Φ_T is a universal scaling function (for the particular transition and values of r , γ , q_0). As an example, we focus on the transition between the LM and ASC phases, for $J > J_c$. A result for the $T = 0$ scaling function Φ_T is shown in Fig. 3. For $\bar{\omega} = \omega/T^* \ll 1$ we have ASC behavior with $\text{Im}\Phi_T \sim |\bar{\omega}|^r$, for $\bar{\omega} \gg 1$ the spectral density follows the quantum-critical power law $|\bar{\omega}|^{-r}$ as predicted above. In both limits the spectrum is particle-hole symmetric (!), however, in the crossover region the asymmetry leads to a large peak for one sign of $\bar{\omega}$ [depending again on $\text{sgn}(q_0 - 1/2)$].

Finally, we mention possible applications of our results. Although we have taken a multichannel large- N limit here, the T-matrix spectral properties of the LM,

ASC, and critical fixed points turn out to apply also to the single-channel case [16]. In most systems there is a finite particle-hole asymmetry, and if Kondo screening is present in a pseudogap system (and r is not too small), the physics will be described by the ASC fixed point [6]. Then, in contrast to the metallic $r = 0$ case, the impurity spectral function does not show a peak at the Fermi level, but at an energy of order $T_K \sim T^*$ (Fig. 3, see also [3]). Interestingly, STM studies of Zn impurities in the cuprate d -wave superconductor BSCCO [9] have shown a large peak in the differential conductance at a small bias of 1.5 meV, and a likely possibility is that this peak arises from the Kondo screening of the impurity-induced moment [17]. The value of $T^* = 15$ K is consistent with NMR studies [7] which show a T_K of order 20–40 K around optimal doping. Last not least, genuine multichannel pseudogap physics may be found in quantum dots coupled to d -wave-superconducting leads, and possibly in heavy-fermion superconductors [13].

The author thanks H. Alloul, R. Bulla, A. Georges, O. Parcollet, A. Polkovnikov, T. Pruschke, and S. Sachdev for invaluable discussions. This research was supported by the DFG through SFB 484.

-
- [1] A. C. Hewson, *The Kondo Problem to Heavy Fermions*, Cambridge University Press, Cambridge (1997).
 - [2] D. Withoff and E. Fradkin, Phys. Rev. Lett. **64**, 1835 (1990); L. S. Borkowski and P. J. Hirschfeld, Phys. Rev. B **46**, 9274 (1992); K. Ingersent and Q. Si, cond-mat/9810226.
 - [3] C. R. Cassanello and E. Fradkin, Phys. Rev. B **53**, 15079 (1996) and **56**, 11246 (1997);
 - [4] K. Chen and C. Jayaprakash, J. Phys.: Condens. Matter **7**, L491 (1995), K. Ingersent, Phys. Rev. B **54**, 11936 (1996).
 - [5] R. Bulla *et al.*, J. Phys.: Condens. Matter **9**, 10463 (1997), **12**, 4899 (2000).
 - [6] C. Gonzalez-Buxton and K. Ingersent, Phys. Rev. B **57**, 14254 (1998).
 - [7] J. Bobroff *et al.*, Phys. Rev. Lett. **83**, 4381 (1999) and **86**, 4116 (2001).
 - [8] D. E. Logan and M. T. Glossop, J. Phys.: Condens. Matter **12**, 985 (2000).
 - [9] E. W. Hudson *et al.*, Science **285**, 88 (1999); S. H. Pan *et al.*, Nature **403**, 746 (2000).
 - [10] O. Parcollet and A. Georges, Phys. Rev. Lett. **79**, 4665 (1997).
 - [11] O. Parcollet *et al.*, Phys. Rev. B **58**, 3794 (1998).
 - [12] P. Nozières and A. Blandin, J. Phys. (Paris) **41**, 193 (1980).
 - [13] D. L. Cox and A. Zawadowski, Adv. Phys. **47**, 599 (1998).
 - [14] D. L. Cox and A. E. Ruckenstein, Phys. Rev. Lett. **71**, 1613 (1993).
 - [15] S. Sachdev, *Quantum Phase Transitions*, Cambridge University Press, Cambridge (1999).
 - [16] M. Vojta and R. Bulla, NRG results, to be published.
 - [17] A. Polkovnikov, S. Sachdev, and M. Vojta, Phys. Rev. Lett. **86**, 296 (2001).